

## Predicting the optoelectronic properties of nanowire films based on control of length polydispersity

Article (Published Version)

Large, Matthew J, Burn, Jake, King, Alice A, Ogilvie, Sean P, Jurewicz, Izabela and Dalton, Alan B (2016) Predicting the optoelectronic properties of nanowire films based on control of length polydispersity. *Scientific Reports*, 6. p. 25365. ISSN 2045-2322

This version is available from Sussex Research Online: <http://sro.sussex.ac.uk/60833/>

This document is made available in accordance with publisher policies and may differ from the published version or from the version of record. If you wish to cite this item you are advised to consult the publisher's version. Please see the URL above for details on accessing the published version.

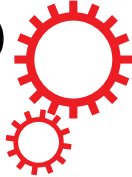
### **Copyright and reuse:**

Sussex Research Online is a digital repository of the research output of the University.

Copyright and all moral rights to the version of the paper presented here belong to the individual author(s) and/or other copyright owners. To the extent reasonable and practicable, the material made available in SRO has been checked for eligibility before being made available.

Copies of full text items generally can be reproduced, displayed or performed and given to third parties in any format or medium for personal research or study, educational, or not-for-profit purposes without prior permission or charge, provided that the authors, title and full bibliographic details are credited, a hyperlink and/or URL is given for the original metadata page and the content is not changed in any way.

# SCIENTIFIC REPORTS



OPEN

## Predicting the optoelectronic properties of nanowire films based on control of length polydispersity

Matthew J. Large<sup>1</sup>, Jake Burn<sup>1</sup>, Alice A. King<sup>1</sup>, Sean P. Ogilvie<sup>1,2</sup>, Izabela Jurewicz<sup>1</sup> & Alan B. Dalton<sup>1,2</sup>

Received: 14 February 2016

Accepted: 15 April 2016

Published: 09 May 2016

We demonstrate that the optoelectronic properties of percolating thin films of silver nanowires (AgNWs) are predominantly dependent upon the length distribution of the constituent AgNWs. A generalized expression is derived to describe the dependence of both sheet resistance and optical transmission on this distribution. We experimentally validate the relationship using ultrasonication to controllably vary the length distribution. These results have major implications where nanowire-based films are a desirable material for transparent conductor applications; in particular when application-specific performance criteria must be met. It is of particular interest to have a simple method to generalize the properties of bulk films from an understanding of the base material, as this will speed up the optimisation process. It is anticipated that these results may aid in the adoption of nanowire films in industry, for applications such as touch sensors or photovoltaic electrode structures.

Indium Tin Oxide (ITO) is a widely used transparent conductive oxide with applications as a transparent electrode material in the vast majority of electronic devices available today. Since the first widespread adoption of touch-screen devices shortly after the turn of the millennium, the price of bulk Indium has increased significantly. Supply uncertainty has also applied pressure to the ITO industry, leading to investigation of alternative materials over the last decade or so. Furthermore, looking toward next generation devices which are anticipated to be curved or flexible, ITO is deemed to be unsuitable due to its brittle crystalline structure and high deposition temperature.

Alternative materials investigated as ITO replacements have included graphene, carbon nanotubes, metal mesh and random metal nanowire films. Of these, silver nanowire (AgNW) films have emerged as the strongest competitor, due to transmittances and conductivities which can match and readily exceed those of ITO.

The rapid adoption of nanowire films in transparent conductor applications requires a robust method for designing materials capable of meeting application-specific performance requirements. These requirements typically include high transmittance and low sheet resistance. Also of importance to displays and sensor applications is low haze (the ratio of diffuse to specular transmittance). Higher haze is a useful feature in photovoltaic applications, where this improves coupling and trapping of light inside the device, leading to increases in device efficiency.

Typically a mathematical expression relating film transmittance  $T$  and sheet resistance  $R_S$  (termed a T-R expression) is used to gauge the relative performance of the transparent electrode. Two established forms for this relation exist at present; the first describes continuous bulk films<sup>1</sup>, and the second describes percolating nanostructured materials<sup>2</sup>;

$$T = \left[ 1 + \frac{1}{\Pi} \left( \frac{Z_0}{R_S} \right)^{\frac{1}{1+n}} \right]^{-2} \quad (1)$$

where  $Z_0$  is the impedance of free space ( $Z_0 = 377 \Omega$ );  $n$  is a percolative exponent describing the power law relation between  $R_S$  and the film thickness;  $\Pi$  is a percolative figure of merit, where higher values couple low values of  $R_S$  to high values of  $T$ .

<sup>1</sup>University of Surrey, Department of Physics, Guildford, GU2 7XH, United Kingdom. <sup>2</sup>University of Sussex, Department of Physics, Brighton, BN1 9RH, United Kingdom. Correspondence and requests for materials should be addressed to M.J.L. (email: m.large@surrey.ac.uk) or A.B.D. (email: a.b.dalton@sussex.ac.uk)

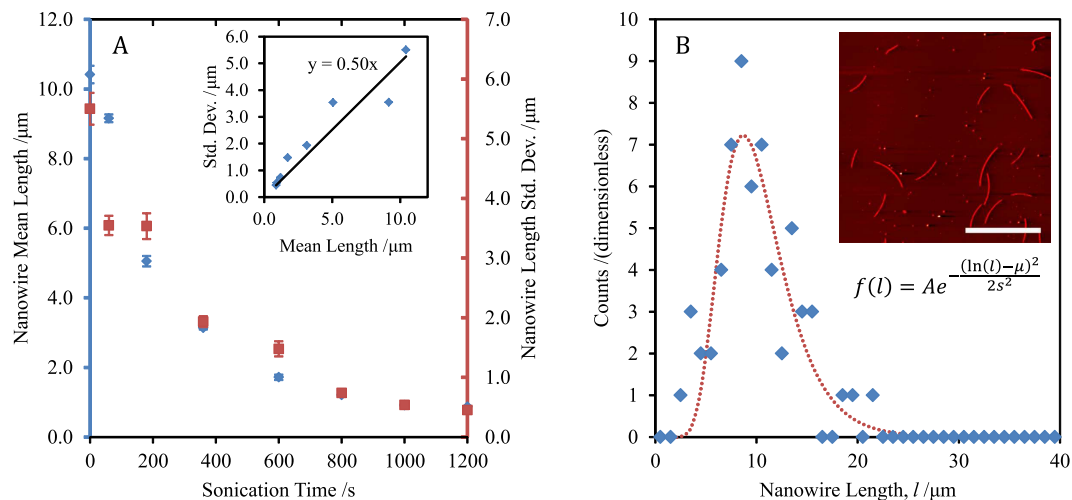


**Figure 1.** (A) Shows how the measured length statistics ( $\langle l \rangle$  (mean length) and  $\sigma$  (standard deviation) vary with sonication time. A Fisherbrand FB15051 bath sonicator with nominal 320 W peak output in swept-frequency mode was used. The inset illustrates the approximate relationship between  $\langle l \rangle$  and  $\sigma$ . (B) Shows a typical length distribution measured from AFM data (a characteristic image is shown in the inset; four different fields are used to compile the histogram data for each sample. The scale bar is 30  $\mu\text{m}$ ). The fitted distribution function is log-normal, with parameters  $\mu = 2.14 \pm 0.01 \mu\text{m}$  and  $s = 0.37 \pm 0.01 \mu\text{m}$  which correspond to a mean length of  $\langle l \rangle = 9.2 \pm 0.1 \mu\text{m}$  and standard deviation of  $\sigma = 3.5 \pm 0.2 \mu\text{m}$  (fitted parameter variances are evaluated using a delete-1 jackknife resampling method<sup>17</sup>).

Prior work presented in the literature has recognised a qualitative relationship between the mean length of silver nanowires and their T-R performance<sup>3-7</sup>.

Ultrasonication has been demonstrated as a technique capable of manipulating the length distribution of high aspect ratio nanoparticles<sup>8,9</sup>. The application of high pressure amplitude acoustic waves to a nanoparticle dispersion induces the formation and growth of cavitation bubbles. These bubbles can be stable, oscillating in phase with the driving acoustic field, or collapse chaotically generating large local temperature increases and local fluid flow rates. It is the latter behavior, known as inertial cavitation, which leads to the process of ultrasonic scission of rod-like nanoparticles<sup>9</sup>.

## Results

Figure 1(A) illustrates the capability of ultrasonication to modify the length distribution of silver nanowires in solution by control of the sonication time. As-received silver nanowire material from a commercial supplier was diluted in IPA to a concentration suitable for spray deposition prior to treatment in a room temperature ultrasonic bath. The initial nanowire population has a diameter of  $d = 30 \pm 4 \text{ nm}$  (measured by TEM), a mean length of  $\langle l \rangle = 10.4 \mu\text{m}$  and a length standard deviation of  $\sigma = 5.5 \mu\text{m}$  (measured by AFM, see Fig. 1(B) for a characteristic measurement). The inset to Fig. 1(A) shows that an approximate relationship is maintained between the standard deviation and mean length.

It has long been understood that the performance of nanowire films as transparent conductors is linked to the length of the nanowires used<sup>3-7</sup>. We develop a modification to the theory given by De *et al.*<sup>2</sup>, described in detail in the Supplementary Information, which clarifies the link between nanowire length statistics and the resulting electro-optical film performance.

From continuum percolation theory we have a percolative scaling relation for film conductivity  $1/R_S$  that depends on the nanowire density measured by the filling factor  $\eta_s$ ;

$$\frac{1}{R_S} = \frac{1}{M'} (\eta_s - \eta_{s,c})^m \quad (2)$$

where  $R_S$  is the sheet resistance;  $M'$  is a material constant;  $m$  is the percolative exponent of conductivity (which has a nominally universal value of  $m = 1.30$  in two dimensions). The filling factor is defined as the total squared length of rods per unit area of the substrate. This measure is convenient since the percolation threshold density,  $\eta_{s,c} = 5.6372 \dots$ <sup>10</sup>, is expected to be universal for all rod-like objects and independent of their length distribution. We can relate  $\eta_s$  to the area fraction  $\phi_s$  (the total projected area of objects per unit area of the substrate) by  $\phi_s = \eta_s d \langle l \rangle / \langle l^2 \rangle$ , and by inversion of equation (2) relate the area fraction to the sheet resistance;

$$\phi_s = \frac{d \langle l \rangle}{\langle l^2 \rangle} \left[ \left( \frac{M'}{R_S} \right)^{\frac{1}{m}} + \eta_{s,c} \right] \quad (3)$$

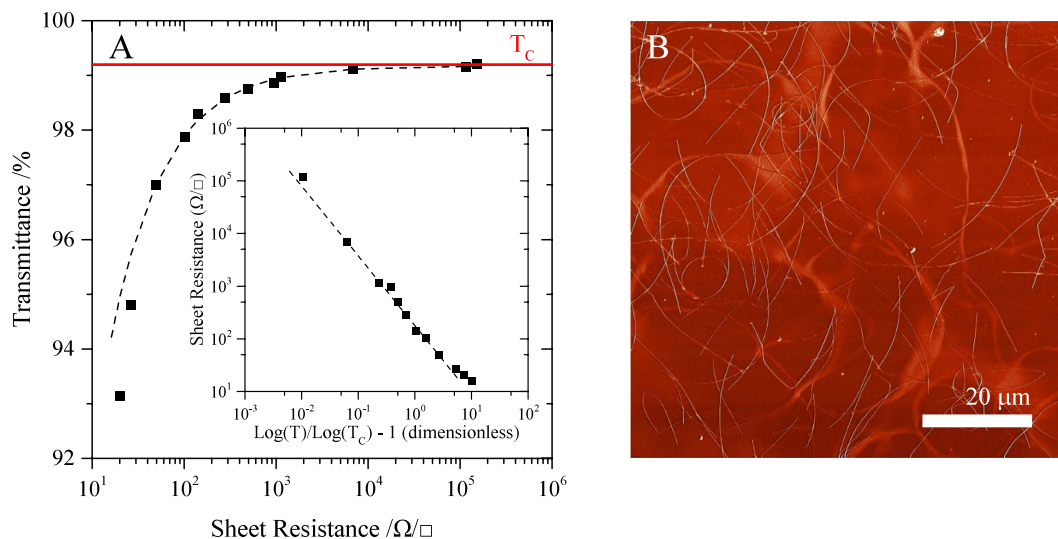


**Figure 2.** (A) shows typical sheet resistance and transmittance data for a film prepared using unsonicated nanowire material. The critical transmittance is calculated to be 99.1%. Equation (5) is fitted to the data, giving fitted values of  $\Pi' = 960$ , and  $m = 1.33 \pm 0.04$ ; the inset shows the same data on a log-log plot of  $R_s$  against  $\log_{10} T / \log_{10} T_c - 1$  (which corresponds to  $\eta_s / \eta_{s,c} - 1$ ). (B) shows a phase-contrast AFM image of a representative silver nanowire network with  $T(550 \text{ nm}) = 98.6\%$  and  $R_s \approx 10 \text{ k}\Omega/\square$ , the scale bar is  $10 \mu\text{m}$ .

We adopt a semi-empirical model of the film transmission in the form of the Beer-Lambert law, and deduce that;

$$T = 10^{-Q_{\text{ext}} \phi_s} \quad (4)$$

where  $T$  is the film transmittance and  $Q_{\text{ext}} = \sigma_{\text{ext}}/d$  is the dimensionless extinction efficiency of the nanowires ( $\sigma_{\text{ext}}$  is the extinction cross-section per unit length). Substitution of equation (3) into equation (4) gives a new T-R expression;

$$T = 10^{-Q_{\text{ext}} \frac{d \langle l \rangle}{l^2} \left[ \left( \frac{M'}{R_s} \right)^{\frac{1}{m}} + \eta_{s,c} \right]} \quad (5)$$

By considering the limit as  $R_s \rightarrow \infty$  we discover a ‘critical transmittance’ term, representing an upper bound on the transmittance of a conducting film;

$$T_c = 10^{-Q_{\text{ext}} \frac{d \langle l \rangle}{l^2} \eta_{s,c}} \quad (6)$$

By considering the complementary limit, where  $R_s$  is small such that  $(M'/R_s)^{1/m} \gg \eta_{s,c}$ , and comparing the first order expansion of equation (5) to that of equation (1), we arrive at a percolative figure of merit comparable to that derived by De *et al.*<sup>2</sup> (see Supplementary Information for details);

$$\Pi' = \frac{2 \left( \frac{Z_0}{M'} \right)^{\frac{1}{m}} \langle l^2 \rangle}{\ln(10) Q_{\text{ext}} d \langle l \rangle} \quad (7)$$

From equation (7) we expect film performance to decrease with decreasing nanowire length (since the term  $\langle l^2 \rangle / \langle l \rangle$  scales with the mean length). We would also expect that larger diameter nanowires should not perform as well for a given length distribution (bearing in mind that the extinction efficiency  $Q_{\text{ext}}$  is monotonic with, but not linear in, the nanowire diameter).

In order to confirm the predicted effect of length distribution on the performance of nanowire films, sonicated material is spray deposited onto glass substrates, with transmittance and sheet resistance values collected between sequential spray passes. Fig. 2(A) shows a typical T-R data series for unsonicated nanowire material. Equation (5) has been fitted to the data with  $m$  and  $M'$  as the only free parameters; the AFM length distribution measurements of Fig. 1 are used in the calculations, along with  $Q_{\text{ext}} = 29.6\%$  (calculated using Lumerical FDTD<sup>11</sup> for nanowires of 30 nm diameter).

By introducing the length statistic  $\langle l^2 \rangle / \langle l \rangle$  as a third fitting parameter it is possible to identify an aspect of the nanowire length distribution given the T-R data alone (provided the nanowire diameter, and therefore extinction properties, are known). Figure 3(A) shows the fitted value of the critical transmittance for nanowire material sonicated for increasing durations, where each data point is an average over three samples. Fig. 3(B) plots the fitted

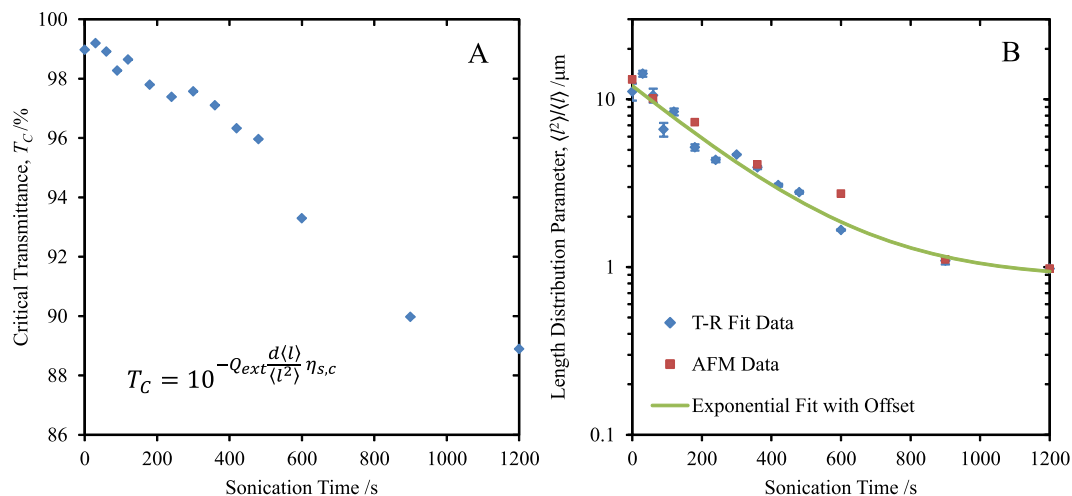


**Figure 3.** (A) Plot of  $T_C$  against sonication time for films formed of sonicated material (the average of three samples is shown). The data are derived by fitting equation (5) to T-R data using the variables  $M'$ ,  $m$  and  $\langle l \rangle^2 / \langle l \rangle$  as fitting parameters. (B) Plot of the fitted parameter  $\langle l^2 \rangle / \langle l \rangle$  against sonication time. The AFM values are derived from the data presented in Fig. 1(A). The fit to the T-R data results is defined by  $f(t) = A \exp(-\alpha t) + c$ , where  $A = 11.2 \mu\text{m}$ ,  $\alpha = 0.0040 \text{ s}^{-1}$  and  $c = 0.85 \mu\text{m}$ , over the 0 to 1200 s range.

value of the length distribution parameter,  $\langle l^2 \rangle / \langle l \rangle$ ; for comparison the values of  $\langle l^2 \rangle / \langle l \rangle$  calculated from the AFM measurements of Fig. 1(A) are shown.

Agreement between the T-R fitted values and the AFM measurements is extremely good. We can suggest that the macroscopic behaviour of transparent conductive films formed from nanowires has a robust dependence on the length distribution of those nanowires, and that manipulation of the nanowire length distribution can be achieved through the use of ultrasonication. We can also infer that the described T-R model correctly captures the effect of variation in the length distribution on the critical transmittance.

The trend fitted to the data in Fig. 3(B) indicates that there exists a limiting value of  $\langle l^2 \rangle / \langle l \rangle$  obtainable using this ultrasonic scission process. This is consistent with the mechanism suggested by Huang<sup>8</sup>, whereby the limiting length  $L_{\text{lim}}$  of nanorods with diameter  $d$  is related to the solvent viscosity  $\eta_{\text{sol}}$ , cavitation bubble radius  $R_i$  and wall collapse rate  $\dot{R}_i$ , and the tensile strength of the material of interest  $\sigma^*$  by;

$$L_{\text{lim}} = \sqrt{\frac{d^2 \sigma^*}{2 \eta_{\text{sol}} \left( \frac{\dot{R}_i}{R_i} \right)}} \quad (8)$$

Utilising the approximate cavitation parameters  $(\dot{R}_i / R_i \approx 10^8 \text{ s}^{-1})^8$  and the nominal viscosity of our dispersing solvent (IPA) at room temperature ( $\eta_{\text{IPA}} \approx 0.002 \text{ Pa} \cdot \text{s}^{12}$ ), and assuming that the length distribution parameters are related as in the inset in Fig. 1(A) (so that  $\langle l^2 \rangle / \langle l \rangle \approx 1.25 \langle l \rangle$ ), we anticipate that  $\lim_{t \rightarrow \infty} \langle l^2 \rangle / \langle l \rangle \approx 0.8 \mu\text{m}$  in excellent agreement with the fitted value of  $0.85 \mu\text{m}$  from Fig. 3.

Figure 4 qualitatively illustrates the ability of solution-phase ultrasonication to tailor the electro-optical properties of deposited nanowire films. Figure 4(A) shows a photograph of a film utilizing unsonicated nanowires with mean length  $\langle l \rangle = 12.4 \mu\text{m}$ , and (B) shows a comparable film produced using sonicated nanowires with mean length  $\langle l \rangle = 1.54 \mu\text{m}$ . Films (A) and (B) have the same sheet resistance ( $60 \Omega / \square$ ), but film (A) has a significantly higher transmittance and lower haze than (B). Both of these points are illustrated by the pixel intensity profile in Fig. 4(C). As can be seen, the contrast between light and dark areas of the image is reduced for the film of Fig. 4(B), indicating higher haze. Also, the average pixel intensity for the film (B) profile is 6% lower than that for film (A).

This type of control may prove useful in situations where optimization of multiple parameters is of interest. For example, sacrificing some transmittance to increase film scattering is a useful feature in photovoltaic transparent electrodes as increased light coupling into, and light trapping within, the device is important<sup>13</sup>. Also, the higher area coverage of nanowires on the surface will enhance the collection efficiency of photo-generated charge carriers at the electrodes.

## Discussion

By evaluating the effect of controlled sonication on the length distribution of AgNWs it is possible to determine a generalized relationship for the macroscale optoelectronic properties of a percolating film derived of such nanowires. We expect that this method can be generalized to any nanowire films for which the nanoscale properties are known, or indeed vice versa. This expression allows for a simple and robust method to determine either film properties from known nanoscale data or the nanoscale properties of a bulk film based on macroscopic T-R measurement series.

The process of ultrasonic scission in this procedure is dependent on nanowire diameter and solvent viscosity<sup>8</sup>, and will likely also be influenced by the dispersion concentration as well as other factors. This gives a broad range

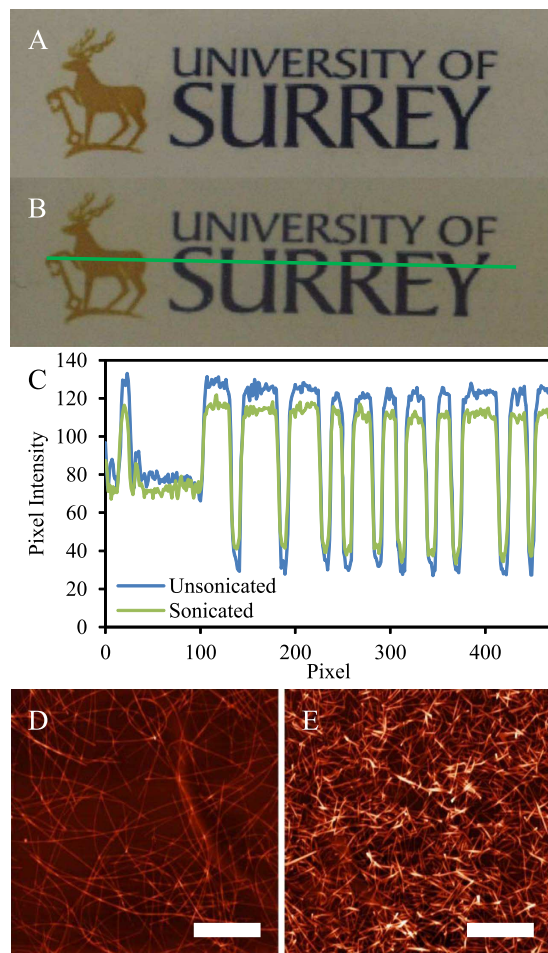


**Figure 4.** (A,B) show photographic images of films sprayed using unsonicated ( $\langle l \rangle = 12.4 \pm 0.1 \mu\text{m}$ ,  $\sigma = 4.5 \pm 0.1 \mu\text{m}$ ) and sonicated ( $\langle l \rangle = 1.54 \pm 0.1 \mu\text{m}$ ,  $\sigma = 0.89 \pm 0.03 \mu\text{m}$ ) nanowires respectively, with a sheet resistance of approximately  $60 \Omega/\square$ . (C) plots the pixel intensities along the line section (green line) shown in Fig. 4(B) for both images (A,B), extracted using ImageJ<sup>16</sup>. Pixel intensities are integers on the range [0,255] representing the equivalent grayscale value at each pixel. (D,E) show representative AFM topography for the films (A,B) respectively; the scale bars are  $5 \mu\text{m}$ .

of control parameters for optimization of film materials, complementing the use of hybrid-type films in transparent electrode applications<sup>14,15</sup>.

## Methods

**Silver nanowire dispersion and ultrasonication.** AgNW dispersions were purchased from a commercial supplier, with an as-received silver concentration in the range of 1–5 mg/mL. The material is used as-received and diluted in IPA at a mass ratio of 0.75:10. Diluted AgNW dispersions were ultrasonicated using a Fisher Scientific FB15051 (nominal ~300 W output) ultrasonic bath in ice. After sonication three drops of the dispersion were spin coated onto microscope cover slips at 3000 rpm for 20 s each. These samples were used to obtain AFM length distribution measurements.

**Spray deposition and sheet resistance measurements.** Diluted AgNW dispersions were deposited on glass microscope slides using a consumer airbrush with a commercial air compressor (Impax IM200-12) set to a back pressure of 5 bar. Parallel bar electrodes were added to the substrates using silver paint (Agar Scientific G3790) and two-point resistance measurements taken using a Keithley 2400 Sourcemeeter.

**UV-Visible spectrophotometry.** UV-Visible spectrophotometry measurements were made using both a Campsec M350 dual beam spectrophotometer and a Shimadzu UV2501PC dual beam spectrophotometer. Measurements were taken of each substrate prior to film deposition.

**Atomic force microscopy.** AFM measurements were performed on an NT-MDT microscope in semi-contact mode using tips with a resonant frequency between 200 and 300 kHz. For length distribution measurements, three  $100 \times 100 \mu\text{m}$  fields were taken for each sample, with the AgNW lengths measured using image analysis software (ImageJ<sup>16</sup>).

## References

- Dressel, M. & Grüner, G. *Electrodynamics of solids: optical properties of electrons in matter*. Ch. 2, 31–46 (Cambridge University Press, 2002).
- De, S., King, P. J., Lyons, P. E., Khan, U. & Coleman, J. N. Size Effects and the Problem with Percolation in Nanostructured Transparent Conductors. *ACS Nano* **4**, 7064–7072, doi: 10.1021/Nn1025803 (2010).
- Lee, P. *et al.* Highly Stretchable and Highly Conductive Metal Electrode by Very Long Metal Nanowire Percolation Network. *Adv Mater* **24**, 3326–3332, doi: 10.1002/adma.201200359 (2012).
- Jiu, J. *et al.* Facile synthesis of very-long silver nanowires for transparent electrodes. *J. Mater. Chem. A* **2**, 6326–6330, doi: 10.1039/c4ta00502c (2014).
- Araki, T. *et al.* Low haze transparent electrodes and highly conducting air dried films with ultra-long silver nanowires synthesized by one-step polyol method. *Nano Res* **7**, 236–245, doi: 10.1007/s12274-013-0391-x (2013).
- Lee, S. J. *et al.* A roll-to-roll welding process for planarized silver nanowire electrodes. *Nanoscale* **6**, 11828–11834, doi: 10.1039/c4nr03771e (2014).
- Bergin, S. M. *et al.* The effect of nanowire length and diameter on the properties of transparent, conducting nanowire films. *Nanoscale* **4**, 1996–2004, doi: 10.1039/C2nr30126a (2012).
- Huang, Y. Y., Knowles, T. P. J. & Terentjev, E. M. Strength of Nanotubes, Filaments, and Nanowires From Sonication-Induced Scission. *Adv Mater* **21**, 3945–3948, doi: 10.1002/adma.200900498 (2009).
- Sesis, A. *et al.* Influence of Acoustic Cavitation on the Controlled Ultrasonic Dispersion of Carbon Nanotubes. *J Phys Chem B* **117**, 15141–15150, doi: 10.1021/Jp410041y (2013).
- Mertens, S. & Moore, C. Continuum percolation thresholds in two dimensions. *Phys Rev E* **86**, 061109, doi: 10.1103/PhysRevE.86.061109 (2012).
- Lumerical Solutions Inc. *FDTD Solutions*, www.lumerical.com/tcad-products/fdtd/ (2015) (Date Accessed: 01/04/2016).
- Yaws, C. L. *Yaws' Handbook of Thermodynamic and Physical Properties of Chemical Compounds*. (Knovel, 2003).
- Preston, C. *et al.* Silver nanowire transparent conducting paper-based electrode with high optical haze. *J Mater Chem C* **2**, 1248–1254, doi: 10.1039/C3tc31726a (2014).
- Jurewicz, I. *et al.* Insulator-Conductor Type Transitions in Graphene-Modified Silver Nanowire Networks: A Route to Inexpensive Transparent Conductors. *Adv Funct Mater*, 7580–7587, doi: 10.1002/adfm.201402547 (2014).
- Liang, J. J. *et al.* Silver Nanowire Percolation Network Soldered with Graphene Oxide at Room Temperature and Its Application for Fully Stretchable Polymer Light-Emitting Diodes. *ACS Nano* **8**, 1590–1600, doi: 10.1021/Nn405887k (2014).
- ImageJ: Image Processing and Analysis in Java, <http://imagej.nih.gov/ij/> (2015) (Date Accessed: 01/04/2016).
- Shao, J. & Tu, D. *The Jackknife and Bootstrap*. (Springer-Verlag, 1995).

## Acknowledgements

The authors would like to gratefully acknowledge funding from M-Solv Ltd and the UK Defence Science and Technology Laboratory (DSTL, contract number DSTLx1000085819). This work was supported by the Engineering and Physical Sciences Research Council (EPSRC, grant numbers EP/K031562/1 and EP/M507775/1).

## Author Contributions

M.L. and J.B. performed the experimental work. M.L. prepared the manuscript with the assistance of A.K., S.O. and I.J.; J.B., A.K., S.O., I.J. and A.D. reviewed the manuscript prior to submission.

## Additional Information

**Supplementary information** accompanies this paper at <http://www.nature.com/srep>

**Competing financial interests:** The authors declare no competing financial interests.

**How to cite this article:** Large, M. J. *et al.* Predicting the optoelectronic properties of nanowire films based on control of length polydispersity. *Sci. Rep.* **6**, 25365; doi: 10.1038/srep25365 (2016).



This work is licensed under a Creative Commons Attribution 4.0 International License. The images or other third party material in this article are included in the article's Creative Commons license, unless indicated otherwise in the credit line; if the material is not included under the Creative Commons license, users will need to obtain permission from the license holder to reproduce the material. To view a copy of this license, visit <http://creativecommons.org/licenses/by/4.0/>